1-2023

Dual Quaternion Relative Dynamics for Gravity Recovery Missions

Ryan Kinzie

Riccardo Bevilacqua

Seo Dongeun

(Preprint) AAS 23-191

DUAL QUATERNION RELATIVE DYNAMICS FOR GRAVITY RECOVERY MISSIONS

Ryan Kinzie*, Riccardo Bevilacqua† and Dongeun Seo‡

A dual quaternion modeling approach is compared to traditional modeling methods for formation flying spacecraft utilized for gravity recovery missions. A modeling method that has traditionally been used for gravity recovery missions is presented which models the motion of two formation flying spacecraft and a test mass. This is followed by the dual quaternion-based formulation for the equations of motion of the twelve degree-of-freedom coupled relative dynamics of formation flying spacecraft and a test mass. Lastly, utilizing data products from the Gravity Recovery and Climate Experiment Follow-On mission, a comparison of these two modeling methods is presented which proves the advantage of the proposed dual quaternion-based modeling approach.

INTRODUCTION

As stated by the Committee on Earth Gravity from Space, measuring Earth's temporal and spatially varying gravity potential is of significant interest to many fields of study, including ocean dynamics, continental water variation, sea-level rise, post-glacial rebound, structure and evolution of the crust and Lithosphere, and mantle dynamics and plumes.[1] Since the Earth is a dynamic system that is constantly changing due to its fluid atmosphere and oceans, distribution of groundwater, snow and ice, and shifting tectonic plates, the mapping of Earth's gravity potential is a continually ongoing process.

For twenty years, the Gravity Recovery and Climate Experiment (GRACE) and GRACE Follow-On (GRACE-FO) missions have provided a means of mapping Earth's gravitational potential by calculating the spherical harmonic coefficients and functions used to model Earth's gravity. Both of these missions' science requirements called for the creation of a long-term gravity model up to spherical harmonic degree 150 to show trends in water storage, mass loss ice sheets, etc., and a temporally varying gravity model up to spherical harmonic degree 70 for sets of average values of the geopotential coefficients over a month or less.[2] However, as stated by Srinivasan et al.,[3] most practical applications require an increase to the temporal and spacial resolutions as well as an increase to the accuracy of the coefficients and functions currently calculated by GRACE-FO. From P. Kornfeld et al. it is stated that the four main contributions to the error of the estimated geopotential parameters for the GRACE-FO mission are intersatellite ranging measurement errors, nongravitational acceleration measurement errors, precision orbit determination errors, temporal and spatial

*Graduate Student, Aerospace Engineering, AIAA Student Member, Embry-Riddle Aeronautical University, Daytona Beach, FL 32114, USA, Email: kinzier@my.erau.edu

†Professor, Aerospace Engineering, AIAA Associate Fellow, Embry-Riddle Aeronautical University, Daytona Beach, FL 32114, USA, Email: bevilacr@erau.edu

‡Associate Professor, Aerospace Engineering, AIAA Member, Embry-Riddle Aeronautical University, Daytona Beach, FL 32114, USA, Email: seod@erau.edu

undersampling, and dealiasing errors.[2] More specifically, two of the contributors to the ranging measurement and precision orbit determination error are attitude knowledge errors and errors in the orbit determination processes.[2] Additionally, for a gravity recovery mission such as GRACE-FO, the relative positions of two spacecraft flying in formation are measured to an accuracy of less than 2 μm by a Laser Ranging Interferometer (LRI).[2] This is significant because any use of the reaction control system thrusters to make attitude adjustments also affect the orbit of the spacecraft and thus changes the relative positions of the two spacecraft flying in formation (rotational and translational coupling). However, even though this coupling is present, traditional dynamics modeling and controller design approaches for gravity recovery missions involves decoupling the translational and rotational dynamics of the formation flying spacecraft and then designing controllers for the rotational and translational subsystems separately.[4–6] This is significant because if the rotational and translational coupling is not considered for the formation flying spacecraft, then the error between the estimated relative positions between the two spacecraft and the actual LRI measurements may be considerable and contribute to the intersatellite ranging measurement errors and attitude knowledge errors. Therefore, since modeling the spacecraft dynamics using dual quaternions does not require decoupling the rotational and translational dynamics of the spacecraft, it is expected that spacecraft models and controllers designed by these methods will result in an increase in performance and/or accuracy over the current methods. Dual quaternions also have the potential to reduce errors in the orbit determination processes since these methods are able to simultaneously and efficiently model the coupled translational and rotational motion of rigid bodies.[7–12] For these reasons, this research has chosen to compare dual quaternions to the traditional modeling approaches for modeling the relative motion of spacecraft used for gravity recovery missions. It is hoped that this and future research will be able to pave the way for new mathematical formulations for modeling formation flying spacecraft that will reduce attitude knowledge errors and errors in the orbit determination processes. This would ultimately improve the accuracy of the spherical harmonic coefficients and functions calculated by gravity recovery missions.

EQUATIONS OF MOTION FORMULATION

In this section the frames of reference for the formation flying spacecraft and test mass are presented followed by the traditional formulation of the equations of motion for the two spacecraft and test mass. Lastly, a dual quaternion-based formulation is presented for the same spacecraft and test mass.

Frames of Reference

The equations of motion formulated here utilize four frames of reference that are illustrated in Figures 1 and 2. The first frame is the Earth Centered Inertial Frame which is denoted by I, followed by the Body-Fixed Frame and the Desired-Frame, which are denoted by B and D, respectively. The Desired Frame is defined by a nadir pointing Z-axis, with the X-axis pointing from the center-of-mass of the target spacecraft through the center of GRACE's K/Ka band antenna, with the Y-axis following from the right hand rule. The Body-Fixed Frame is fixed to the center-of-mass of the chaser spacecraft and is identically co-aligned with the Desired Frame. The relative position vector between the Body-Fixed Frame and the Desired Frame is denoted as $\bar{r}_{B/D}$ and the position vectors between the Inertial Frame and the Body-Fixed Frame and the Inertial Frame and the Desired Frame are denoted by $\bar{r}_{B/I}$ and $\bar{r}_{D/I}$, respectively. The Test Mass Frame is denoted by TM which is defined the same as the Body-Fixed Frame, but is instead centered on the center-of-mass of the

chaser spacecraft's test mass. Lastly, the relative position vector between the Test Mass Frame and the Body-Fixed Frame is denoted as $\bar{r}_{TM/B}$ and the position vector between the Inertial Frame and the Test Mass Frame is denoted by $\bar{r}_{TM/I}$.

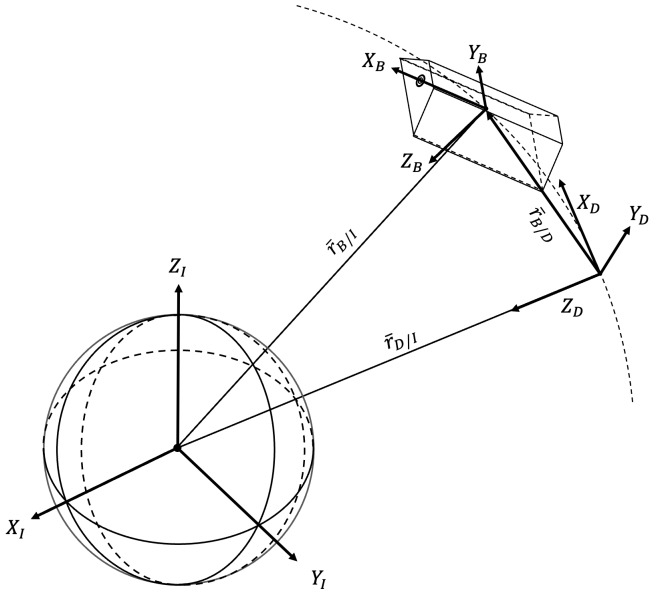

Figure 1. Spacecraft Frames of Reference

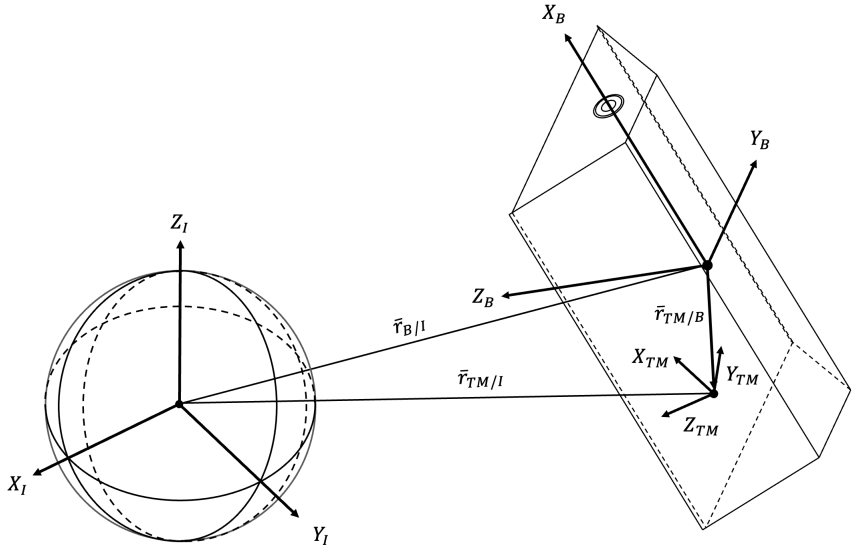

Figure 2. Spacecraft Frames of Reference with Test Mass

Traditional Formulation

The traditional method for formulating the equations of motion for formation flying spacecraft used for gravity recovery missions is presented in Wang et al.,[5] which formulates the translational motion and rotational motion of the spacecraft separately. The translational equations of motion is presented as,

$$\ddot{\bar{r}}^I_{D/I} = \bar{a}^I_g + \bar{a}^I_{J2} \tag{1}$$

where $\bar{a}^D_g$ is the acceleration due to gravity, and $\bar{a}^I_{J2}$ is the acceleration due to J2 perturbations, both resolved in the Inertial Frame. The equations for these follow as,

$$\bar{a}^I_g = -\frac{\mu}{\left\|\bar{r}^I_{D/I}\right\|^3}\bar{r}^I_{D/I}$$

and,

$$\bar{a}^I_{J2} = -\frac{3}{2}\frac{\mu J_2 R_e^2}{\left\|\bar{r}^I_{D/I}\right\|^5}\begin{bmatrix} r_x - \frac{5r_x(r_z)^2}{\left\|\bar{r}^I_{D/I}\right\|^2} \\ r_y - \frac{5r_y(r_z)^2}{\left\|\bar{r}^I_{D/I}\right\|^2} \\ 3r_z - \frac{5(r_z)^3}{\left\|\bar{r}^I_{D/I}\right\|^2} \end{bmatrix}$$

where $\bar{r}^I_{D/I} = [r_x, r_y, r_z]^T$, J_2 is the coefficient representing the effect of the Earth's oblateness, R_e is Earth's mean equatorial radius, and μ is Earth's gravitational parameter. The rotational dynamics are then formulated as,[5]

$$\dot{\bar{\omega}}^D_{D/I} = \left(I^D\right)^{-1}\left[\bar{\tau}^D - \bar{\omega}^D_{D/I} \times \left(I^D\bar{\omega}^D_{D/I}\right)\right] \tag{2}$$

where $\bar{\omega}^D_{D/I}$ is the angular velocity of the Desired Frame with respect to the Inertial Frame, resolved in the Desired Frame, I^D is the moment of inertia of the target spacecraft with respect to the Desired Frame, and $\bar{\tau}^D$ is the externally applied torque on the spacecraft. It is also worth noting that $\dot{\bar{\omega}}^D_{D/I}$ denotes the time derivative of the angular velocity, expressed in the Desired Frame. For this model, the externally applied torque on the spacecraft is simply equivalent to the gravity gradient torque,

$$\bar{\tau}^D = \bar{\tau}^D_{\nabla g} = \frac{3\mu\bar{r}^D_{D/I}}{\left\|\bar{r}^D_{D/I}\right\|^5} \times I^D\bar{r}^D_{D/I}$$

The differential equation of the attitude quaternion used for describing the rotational position of the target spacecraft is then found by,

$$\dot{q}_{D/I} = \frac{1}{2}\left(\bar{\omega}^D_{D/I}\right)^\times q_{D/I} \tag{3}$$

where $(.)^\times$ denotes the skew operator,

$$\left(\bar{\omega}^D_{D/I}\right)^\times = \begin{bmatrix} 0 & \omega_z & -\omega_y & \omega_x \\ -\omega_z & 0 & \omega_x & \omega_y \\ \omega_y & -\omega_x & 0 & \omega_z \\ -\omega_x & -\omega_y & -\omega_z & 0 \end{bmatrix}$$

The equations of motion of the Body-Fixed Frame and the Test Mass Frame have the same formulation as Eq. (1) through Eq. (3), with the appropriate variables being resolved in the Body-Fixed Frame and the Test Mass Frame instead of the Desired Frame.

Since the equations of motion formulated using the method presented above decouple the rotational and translational motion of the spacecraft, any adjustments to the attitude of the spacecraft may increase the error between the estimated relative positions of the two spacecraft and the actual LRI measurements. This may contribute to the intersatellite ranging measurement errors, and attitude knowledge errors, which would ultimately have the potential to decrease the accuracy of the spherical harmonic coefficients and functions calculated by gravity recovery missions.

Dual Quaternion Formulation

A dual quaternion may be comprised of both quaternions and vector quaternions, where a vector quaternion is a quaternion with a scalar part zero, and a vector part nonzero. In this research a dual quaternion is denoted with $\hat{\cdot}$ over a variable, such as $\hat{q} = q_r + \epsilon q_d$ where q_r is referred to the real part of $\hat{q}$, and q_d is referred to as the dual part of $\hat{q}$. Here, ϵ is the dual unit and is defined to be nilpotent ($\epsilon^2 = 0$ and $\epsilon \neq 0$), which is analogous to a complex number, where the complex part is denoted canonically by i or j.[9] The unit dual quaternion is defined as,[7] $\hat{1} = \left[1, \bar{0}^T\right]^T + \epsilon \left[0, \bar{0}^T\right]^T$ and the zero quaternion is defined as, $\hat{0} = \left[0, \bar{0}^T\right]^T + \epsilon \left[0, \bar{0}^T\right]^T$. Additionally, dual quaternion algebra is comprised of a series of operators which are presented in Table 1. In this table it is import to note that a_r, a_d, b_r, and b_d are all quaternions, and therefore any operation depicted by these variables are the canonical quaternion operations. For example, $a_r b_r$ is quaternion multiplication, a_r^* is the quaternion conjugate, etc..

Operator	Action
Addition	$\hat{a} + \hat{b} = (a_r + b_r) + \epsilon (a_d + b_d)$
Multiplication	$\hat{a}\hat{b} = a_r b_r + \epsilon (a_r b_d + a_d b_r)$
Scaler Multiplication	$\lambda \hat{a} = \lambda a_r + \epsilon (\lambda a_d)$
Matrix Multiplication	$M\hat{a} = (M_{11} a_r + M_{12} a_d) + \epsilon (M_{21} a_r + M_{22} a_d)$
Circle Product	$\hat{a} \circ \hat{b} = a_r \cdot b_r + a_d \cdot b_d$
Cross Product	$\hat{a} \times \hat{b} = (a_r \times b_r) + \epsilon (a_r \times b_d + a_d \times b_r)$
Conjugate	$\hat{a}^* = a_r^* + \epsilon a_d^*$
Norm	$\|\hat{a}\| = \sqrt{\hat{a} \circ \hat{a}}$
Swap	$\hat{a}^s = a_d + \epsilon a_r$

Table 1. Dual Quaternion Operators

To formulate the equations of motion of the Desired Frame, Filipe and Tsioas[13] explain that the six degree-of-freedom rigid body dynamics formulated with dual quaternions takes the form of:

$$\dot{\hat{\omega}}^D_{D/I} = \left(\left(M^D\right)^{-1} \left[\hat{f}^D - \left(\hat{\omega}^D_{D/I} \times \left(M^D \left(\hat{\omega}^D_{D/I} \right)^s \right) \right) \right] \right)^s \tag{4}$$

where, M^D is the dual inertia matrix of the target spacecraft, $\hat{f}^D$ is the dual force referenced from the spacecraft's center-of-mass, and $\hat{\omega}^D_{D/I}$ is the dual velocity of the Desired Frame relative to the Inertial Frame, expressed in the Desired Frame. Here, M^D will take the form of:

$$M^D = \begin{bmatrix} 1 & 0^{1\times3} & 0 & 0^{1\times3} \\ 0^{3\times1} & m^D I^{3\times3} & 0^{3\times1} & 0^{3\times3} \\ 0 & 0^{1\times3} & 1 & 0^{1\times3} \\ 0^{3\times1} & 0^{3\times3} & 0^{3\times1} & I^D \end{bmatrix} \tag{5}$$

where $I^{3\times3}$ denotes a 3×3 identity matrix, and m^D is the mass of the target spacecraft. Then, the pose of the Desired Frame, $\hat{q}_{D/I}$, is found by the dual quaternion differential equation:[13]

$$\dot{\hat{q}}_{D/I} = \frac{1}{2}\hat{q}_{D/I}\hat{\omega}^D_{D/I} \tag{6}$$

which allows us to solve for the position of the Desired Frame with respect to the Inertial Frame, $\bar{r}^D_{D/I}$, by,

$$\hat{q}_{D/I} = q_{D/I} + \epsilon\frac{1}{2}q_{D/I}r^D_{D/I}$$

since, $r^D_{D/I} = \left[0, \left(\bar{r}^D_{D/I}\right)^T\right]^T$,

$$r^D_{D/I} = 2q^{-1}_{D/I}q_{D/I_d}$$

where, q_{D/I_d} is the dual part of $\hat{q}_{D/I}$. The dual force will take the form of, $\hat{f}^D = f^D + \epsilon\tau^D$ where f^D and τ^D denote the total force and total torque, respectively. The dual force may also be expressed as a summation of the gravitational effects on the satellite,[8]

$$\hat{f}^D = \hat{f}^D_g + \hat{f}^D_{J_2} + \hat{f}^D_{\nabla g}$$

where, $\hat{f}^D_g$ is the gravitational force, $\hat{f}^D_{J_2}$ is the J_2 perturbation force, and $\hat{f}^D_{\nabla g}$ is the gravity gradient torque. The gravitational force will then take the form of $\hat{f}^D_g = M^D \star \hat{a}^D_g$ where,

$$\hat{a}^D_g = \begin{bmatrix} 0 \\ -\frac{\mu}{\left\|\bar{r}^D_{D/I}\right\|^3}\bar{r}^D_{D/I} \end{bmatrix} + \epsilon \begin{bmatrix} 0 \\ \bar{0} \end{bmatrix}$$

Then, the perturbation force is expressed as $\hat{f}^D_{J_2} = M^D \star \hat{a}^D_{J_2}$where,

$$\hat{a}^D_g = \left[\hat{q}^*_{D/I}\left(\begin{bmatrix} 0 \\ \bar{a}^I_{J_2} \end{bmatrix} + \epsilon \begin{bmatrix} 0 \\ \bar{0} \end{bmatrix}\right)^s \hat{q}_{D/I}\right]^s$$

Lastly, the gravity gradient torque may be written as,

$$\hat{f}^D_{\nabla g} = \frac{3\mu\hat{r}^D_{D/I}}{\left\|\hat{r}^D_{D/I}\right\|^5} \times M^D\left(\hat{r}^D_{D/I}\right)^s$$

The relative pose between the Body-Fixed Frame and Desired Frame formulated with dual quaternions, $\hat{q}_{B/D}$, is similar to Eq. (6) and is formulated as,

$$\dot{\hat{q}}_{B/D} = \frac{1}{2}\hat{q}_{B/D}\hat{\omega}^B_{B/D} \tag{7}$$

where $\hat{\omega}^B_{B/D}$ is the relative dual velocity between the target and chaser spacecraft. Yang and Stoll derives the six degree-of-freedom coupled dual quaternion relative dynamics of the Body-Fixed Frame relative to the Desired Frame as,[8]

$$\dot{\hat{\omega}}^B_{B/D} = \left((M^B)^{-1}\left[\hat{f}^B - \left(\hat{\omega}^B_{B/D} + \hat{\omega}^B_{D/I}\right) \times M^B\left(\left(\hat{\omega}^B_{B/D}\right)^s + \left(\hat{\omega}^B_{D/I}\right)^s\right)\right.\right.$$
$$\left.\left. - M^B \star \left(\hat{q}^*_{B/D}\dot{\hat{\omega}}^D_{D/I}\hat{q}_{B/D}\right) - M^B\left(\hat{\omega}^B_{D/I} \times \hat{\omega}^B_{B/D}\right)^s\right]\right)^s \tag{8}$$

where, $\hat{\omega}^B_{D/I}$ is the dual velocity of the Desired Frame with respect to the Inertial Frame expressed in the Body-Fixed Frame, and M^B is the same as the dual inertia matrix in Eq. (5) with elements expressed in the Body-Fixed Frame for the chaser spacecraft. Lastly, we find $\hat{\omega}^B_{D/I}$ by,

$$\hat{\omega}^B_{D/I} = \hat{q}^*_{B/D}\hat{\omega}^D_{D/I}\hat{q}_{B/D}$$

Additionally, as stated by Yang and Stoll[8] $\hat{q}_{B/D} = \hat{q}^*_{D/I}\hat{q}_{B/I}$, therefore we are able to solve for the pose of the Body-Frame with respect to the inertial frame, $\hat{q}_{B/I}$, with the equation,

$$\hat{q}_{B/I} = \hat{q}_{D/I}\hat{q}_{B/D}$$

The equations of the motion for the relative dynamics of the Test Mass Frame relative to the Body-Fixed Frame are the same as Eq. (7) and Eq. (8) but with every variable appropriately resolved in either the Test Mass Frame or the Body Fixed Frame. Additionally, the summation of dual forces on the test mass, $\hat{f}^{TM}$, consists of the same terms as the dual force on the spacecraft, with the inclusion of the additional term $\hat{f}^{TM}_{coupled}$, which models the dual forces that result from the spacecraft's changing gravitational and magnetic field which act on the test mass,[14]

$$\hat{f}^{TM} = \hat{f}^{TM}_g + \hat{f}^{TM}_{J_2} + \hat{f}^{TM}_{\nabla g} + \hat{f}^{TM}_{coupled}$$

This coupled dual force term is found by combining the force, $\bar{F}_S$, and moment, $\bar{M}_S$, that result from multiplying the relative position and attitude of the test mass, $\bar{r}_{TM/B}$ and $\bar{\vartheta}_{TM/B}$, respectively, to a stiffness matrix, $K_s \in \mathbb{R}^{6\times6}$, which is described in Vidano et al.,[14]

$$\begin{bmatrix} \bar{F}_S \\ \bar{M}_S \end{bmatrix} = K_S \begin{bmatrix} \bar{r}^B_{TM/B} \\ \bar{\vartheta}_{TM/B} \end{bmatrix}$$

$$\hat{f}^{TM}_{coupled} = \begin{bmatrix} 0 \\ \bar{F}_S \end{bmatrix} + \epsilon \begin{bmatrix} 0 \\ \bar{M}_S \end{bmatrix}$$

where

$$r^B_{TM/B} = 2q_{TM/B_d}q^{-1}_{TM/B}$$

since,

$$\hat{q}_{TM/B} = q_{TM/B} + \epsilon\frac{1}{2}r^B_{TM/B}q_{TM/B}$$

and, $r^B_{TM/B} = \left[0, \left(\bar{r}^B_{TM/B}\right)^T\right]^T$, where, q_{TM/B_d} is the dual part of $\hat{q}_{TM/B}$. To find $\bar{\vartheta}_{TM/B}$, we consider the linearized quaternion rotational matrix, which is equal to a small change in the rotational matrix, $[\delta T]^{BL}$, multiplied to its previous iteration, $[T]^{BL}_{i-1}$,[15]

$$[T]^{BL} = [\delta T]^{BL}[T]^{BL}_{i-1}$$

Here, $[\delta T]^{BL}$ is equivalent to the small angle approximation of an $\hat{i}, \hat{j}, \hat{k}$ rotational matrix using Euler Angles, where ψ is roll, θ is pitch, and ϕ is yaw angles, respectively.

$$[\delta T]^{BL} \approx \begin{bmatrix} 1 & \delta\phi & -\delta\theta \\ -\delta\phi & 1 & \delta\psi \\ \delta\theta & -\delta\psi & 1 \end{bmatrix}$$

Then, $[T]_{i-1}^{BL}$ is given by,

$$[T]_{i-1}^{BL} = \begin{bmatrix} T_{i-1_{11}} & T_{i-1_{12}} & T_{i-1_{13}} \\ T_{i-1_{21}} & T_{i-1_{22}} & T_{i-1_{23}} \\ T_{i-1_{31}} & T_{i-1_{32}} & T_{i-1_{33}} \end{bmatrix} = \begin{bmatrix} 1 & 0 & 0 \\ 0 & 1 & 0 \\ 0 & 0 & 1 \end{bmatrix}$$

Therefore, the linearization of $[T]^{BL}$ follows as,

$$[T]^{BL} = \begin{bmatrix} 1 & \delta\phi & -\delta\theta \\ -\delta\phi & 1 & \delta\psi \\ \delta\theta & -\delta\psi & 1 \end{bmatrix}$$

Additionally since we know the form $[T]^{BL}$ takes with quaternions,

$$[T]^{BL} = \begin{bmatrix} q_0^2 + q_1^2 - q_2^2 - q_3^2 & 2\left(q_1 q_2 + q_0 q_3\right) & 2\left(q_1 q_3 - q_0 q_2\right) \\ 2\left(q_1 q_2 - q_0 q_3\right) & q_0^2 - q_1^2 + q_2^2 - q_3^2 & 2\left(q_2 q_3 + q_0 q_1\right) \\ 2\left(q_1 q_3 + q_0 q_2\right) & 2\left(q_2 q_3 - q_0 q_1\right) & q_0^2 - q_1^2 - q_2^2 + q_3^2 \end{bmatrix}$$

we can state that,

$$\bar{\vartheta}_{TM/B} = \begin{bmatrix} \delta\psi \\ \delta\theta \\ \delta\phi \end{bmatrix} = 2 \begin{bmatrix} q_2 q_3 + q_0 q_1 \\ q_1 q_3 + q_0 q_2 \\ q_1 q_2 + q_0 q_3 \end{bmatrix}$$

The above provides us with a full formulation for the coupled relative motion of two Earth orbiting spacecraft formulated with dual quaternions, with the spacecraft - test mass coupling included.

SIMULATIONS AND DISCUSSION

In this section the comparison between the traditional uncoupled equations of motion and the dual quaternion equations of motion for modeling the relative dynamics of the two spacecraft is presented. The translational positions of both the target spacecraft and the chaser spacecraft are of the most interest for this research, since these are the states that are affected when the coupling of the equations of motion of the spacecraft changes. To make this comparison, the ECIF positions of both GRACE C and GRACE D spacecraft from the Level-1B GRACE-FO data products are utilized. The data from the GRACE C spacecraft was utilized for the Desired Frame, and the data from the GRACE D spacecraft was utilized for the Body-Fixed Frame. This allowed for a comparison of the accuracy of the dual quaternion modeling approach verses the traditional uncoupled modeling approach using Eq. (9) and Eq. (10),

$$\left(r_{D/I}^{I}\right)_{\text{Error}} = \left\| \left(\bar{r}_{D/I}^{I}\right)_{\text{GRACE C}} - \left(\bar{r}_{D/I}^{I}\right)_{\text{UC}} \right\| - \left\| \left(\bar{r}_{D/I}^{I}\right)_{\text{GRACE C}} - \left(\bar{r}_{D/I}^{I}\right)_{\text{DQ}} \right\| \tag{9}$$

$$\left(r^I_{B/I}\right)_{\text{Error}} = \left\|\left(\bar{r}^I_{B/I}\right)_{\text{GRACE D}} - \left(\bar{r}^I_{B/I}\right)_{\text{UC}}\right\| - \left\|\left(\bar{r}^I_{B/I}\right)_{\text{GRACE D}} - \left(\bar{r}^I_{B/I}\right)_{\text{DQ}}\right\| \tag{10}$$

where $(.)_{\text{GRACE C}}$ denotes that the respective variable is a data product of the GRACE C spacecraft, $(.)_{\text{GRACE D}}$ denotes that the respective variable is a data product of the GRACE D spacecraft, and $(.)_{\text{DQ}}$ and $(.)_{\text{UC}}$ denote that corresponding vector was obtained using either the dual quaternion (DQ) simulation, or the traditional uncoupled (UC) simulation. The initial conditions for both the dual quaternion and uncoupled simulations were obtained by using the GRACE C and GRACE D data products.

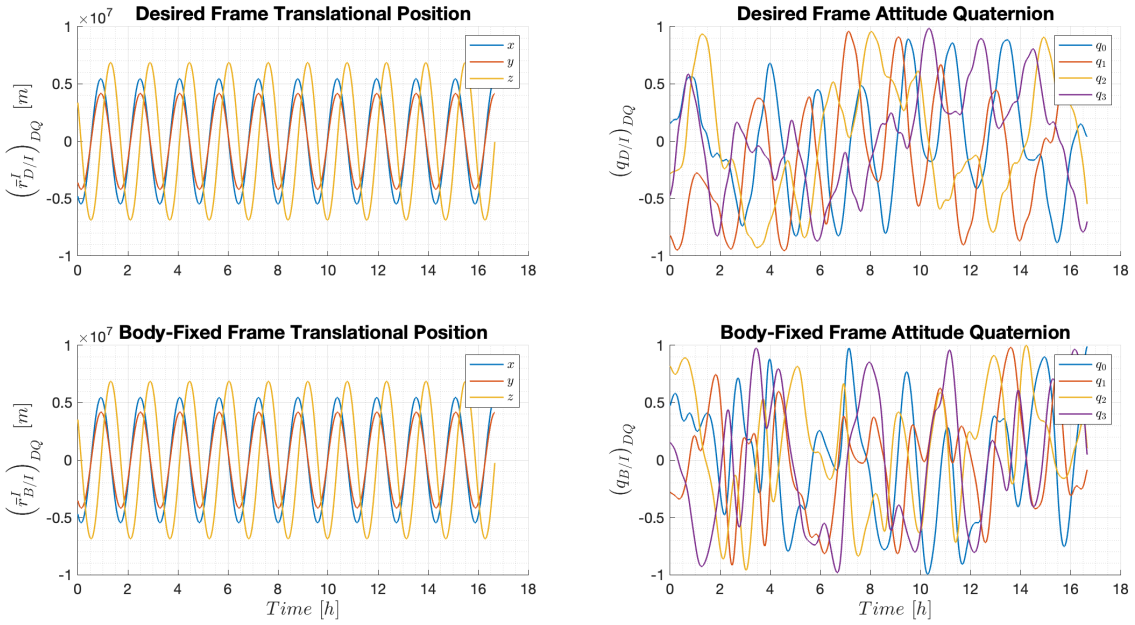

Figure 3. Dual Quaternion Simulation Results

Figure 3 presents the results of Eq. (9) and Eq. (10). From this figure it is clear that $\left(r^I_{D/I}\right)_{\text{Error}}$ and $\left(r^I_{B/I}\right)_{\text{Error}}$ continually increase with time, which means that the error between the dual quaternion modeling approach and the GRACE-FO data products is less than the error between the traditional uncoupled modeling approach and the data products. As expected, this proves that the dual quaternion modeling approach is able to more accurately model the dynamics of both spacecraft. From this figure we can also see that for the Body-Fixed Frame, the error between the two modeling

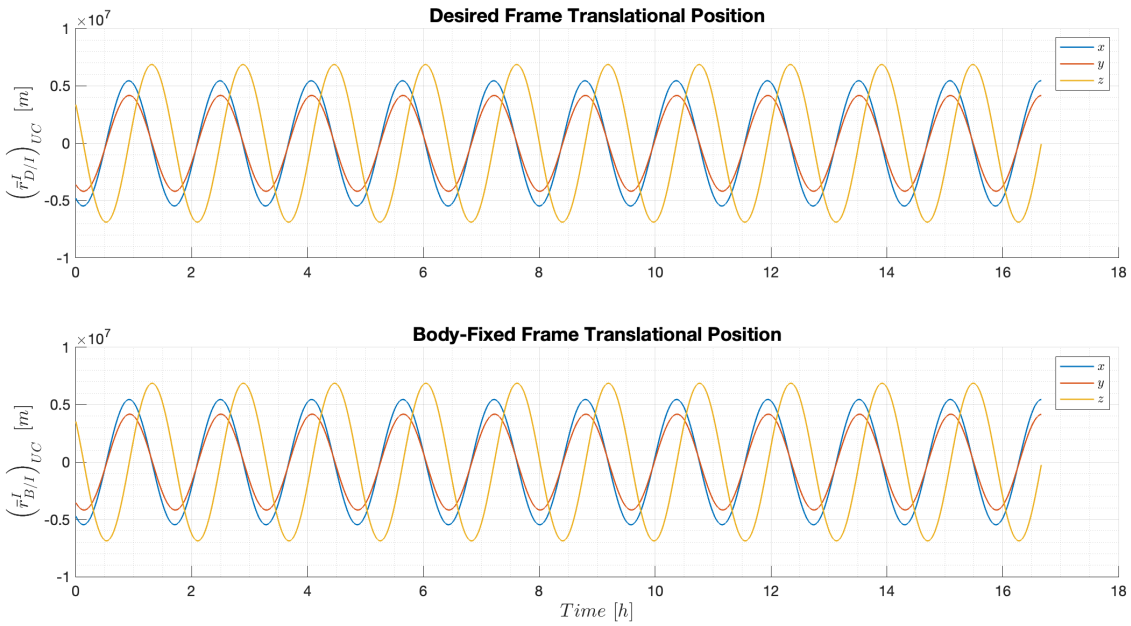

Figure 4. Traditional Simulation Results

approaches reached 1 meter just after 15 hours, which yields an acceleration difference of approximately ~ 340.2 pm/s^2. This is significant because it proves that the dual quaternion approach is able to directly improve estimations of the spacecraft's accelerations on the order of hundreds of picometers per second per second, which may be significant for future gravity recovery missions that seek to improve the spherical harmonic coefficients and functions beyond the current long-term gravity model spherical harmonic degree 150 and temporally varying gravity model spherical harmonic degree 70. Additionally, these simulations don't include external torques beyond gravity gradient torque. During a real mission more external torques would act on the spacecraft, which means that the difference in error will only increase between the dual quaternion model and the uncoupled model. Therefore, an increase in accuracy on the order of hundreds of picometers per second per second is the minimum increase in estimations of the spacecraft's acceleration that would directly result from modeling the relative motion of a gravity recovery spacecraft using dual quaternions.

These results also imply direct improvements to the estimated error between the relative positions between the two spacecraft and the actual LRI measurements as well as improvements to orbit determination processes. These improvements would reduce intersatellite ranging measurement errors and attitude knowledge errors, thus ultimately improving the accuracy of the spherical harmonic coefficients and functions calculated by gravity recovery missions.

CONCLUSION

This research successfully modeled the dynamics of formation flying spacecraft used for gravity recovery missions using both dual quaternions, and the traditional modeling method of decoupling the translational and rotational dynamics. Additionally, by utilizing data products from the Gravity Recovery and Climate Experiment Follow-On mission, it was proven that the estimations of a for-

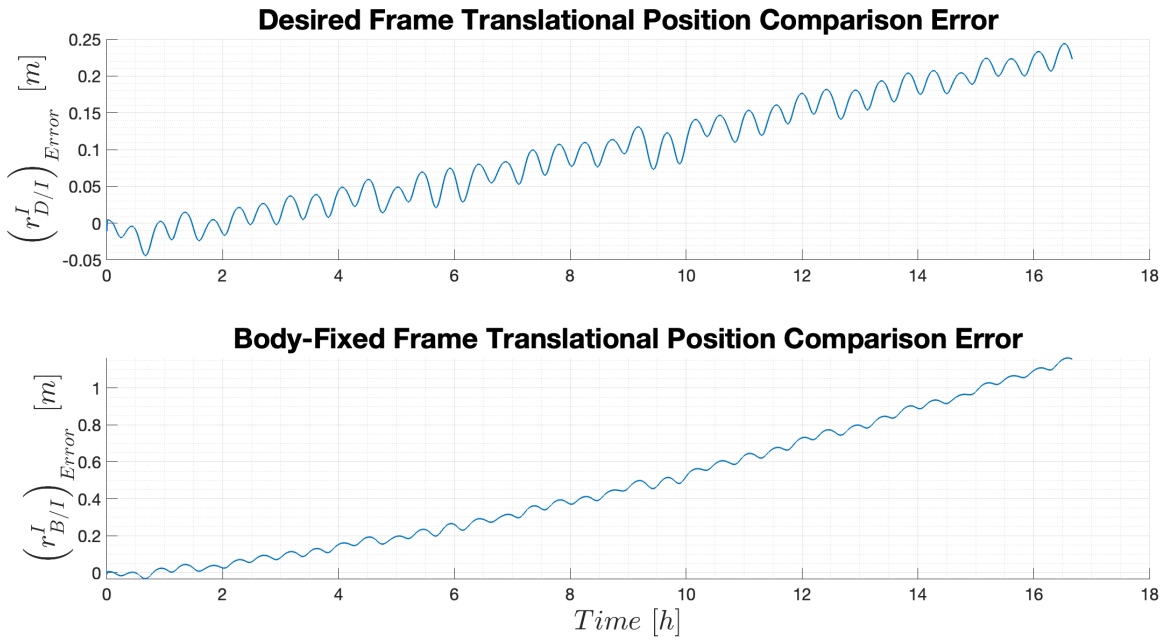

Figure 5. Translational Position Error

mation flying spacecraft's acceleration will be improved by a minimum of hundreds of picometers per second per second by utilizing the relative dual quaternion modeling approach presented here. Additionally, these results also imply direct improvements to the orbit determination process and relative position estimation errors.

Future research will investigate controllers designed from dual quaternions, which will be compared against traditional controllers designed by decoupling the translational and rotational dynamics of the spacecraft and then designing separate controllers for the rotational and translational subsystems.[4–6] Since modeling the spacecraft dynamics using dual quaternions does not require decoupling the rotational and translational dynamics of the spacecraft, it is expected that controllers designed by this method will result in an increase in performance and/or accuracy over the traditional controller designs, which would further improve the accuracy of the spherical harmonic coefficients and functions calculated by future gravity recovery missions.

REFERENCES

[1] N. R. Council *et al.*, *Satellite gravity and the geosphere: contributions to the study of the solid Earth and its fluid envelopes*. National Academies Press, 1997.

[2] R. P. Kornfeld, B. W. Arnold, M. A. Gross, N. T. Dahya, W. M. Klipstein, P. F. Gath, and S. Bettadpur, "GRACE-FO: the gravity recovery and climate experiment follow-on mission," *Journal of spacecraft and rockets*, Vol. 56, No. 3, 2019, pp. 931–951.

[3] M. Srinivasan, M. Rodell, J. T. Reager, L. Rogers, and B. Doorn, "Mass Change Mission Applications–Assessing user needs for the next NASA Mass Change Designated Observable (MCDO) mission," *AGU Fall Meeting 2019*, AGU, 2019.

[4] J. Herman, D. Presti, A. Codazzi, and C. Belle, "Attitude control for GRACE," *18th International Symposium on Space Flight Dynamics*, Vol. 548, 2004, p. 27.

[5] F. Wang, *Study on center of mass calibration and K-band ranging system calibration of the GRACE mission*. The University of Texas at Austin, 2003.

[6] Y. Mashtakov, M. Ovchinnikov, F. Wöske, B. Rievers, and M. List, "Attitude determination & control system design for gravity recovery missions like GRACE," *Acta astronautica*, Vol. 173, 2020, pp. 172–182.

[7] D. Seo, "Fast adaptive pose tracking control for satellites via dual quaternion upon non-certainty equivalence principle," *Acta Astronautica*, Vol. 115, 2015, pp. 32–39.

[8] J. Yang and E. Stoll, "Adaptive sliding mode control for spacecraft proximity operations based on dual quaternions," *Journal of Guidance, Control, and Dynamics*, Vol. 42, No. 11, 2019, pp. 2356–2368.

[9] B. Kenwright, "A beginners guide to dual-quaternions: what they are, how they work, and how to use them for 3D character hierarchies," 2012.

[10] B. McCann and M. Nazari, "Control and maintenance of fully-constrained and underconstrained rigid body motion on Lie groups and their tangent bundles," *Journal of Geometric Mechanics*, Vol. 14, No. 1, 2022, p. 29.

[11] M. Nazari, M. Maadani, E. A. Butcher, and T. Yucelen, "Morse-Lyapunov-based control of rigid body motion on TSE (3) via backstepping," *2018 aiaa guidance, navigation, and control conference*, 2018, p. 0602.

[12] M. Maadani and E. A. Butcher, "Consensus Control of Rigid Body Spacecraft in Orbital Relative Motion using TSE (3) and Exponential Coordinates," *The Journal of the Astronautical Sciences*, 2022, pp. 1–28.

[13] N. Filipe and P. Tsiotras, "Simultaneous position and attitude control without linear and angular velocity feedback using dual quaternions," *2013 American control conference*, IEEE, 2013, pp. 4808–4813.

[14] S. Vidano, C. Novara, M. Pagone, and J. Grzymisch, "The LISA DFACS: Model Predictive Control design for the test mass release phase," *Acta Astronautica*, 2022.

[15] T. Barfoot, J. R. Forbes, and P. T. Furgale, "Pose estimation using linearized rotations and quaternion algebra," *Acta Astronautica*, Vol. 68, No. 1-2, 2011, pp. 101–112.